International Research Journal in Global Engineering and Sciences. (IRJGES)
ISSN : 2456-172X | Vol. 1, No. 4, January, 2017 | Pages 39-51

Measurement & Control of Torque and speed of Induction Machines

Lithesh.J[1], Dr.Mahesh.K[2], Dr.Sainarayanan[3]
Department of Electrical and Electronics Engineering New Horizon College of Engineering, Bangalore.

Abstract: The aim of this research project was to develop a vector controlled induction motor drive operating without a speed or position sensor but having a dynamic performance comparable to a sensored vector drive. The methodology was to detect the motor speed from the machine rotor slot harmonics using digital signal processing and to use this signal to tune a speed estimator and thus reduce or eliminate the estimator's sensitivity to parameter variations. Derivation of a speed signal from the rotor slot harmonics using a Discrete Fourier Transform-based algorithm has yielded highly accurate and robust speed signals above machine frequencies of about 2 Hz and independent of machine loads. The detection, which has been carried out using an Intel i860 processor in parallel with the main vector controller, has been found to give predictable and consistent results during speed transient conditions. The speed signal obtained from the rotor slot harmonics has been used to tune a Model Reference Adaptive speed and flux observer, with the resulting sensor less drive operating to be steady state speed accuracies down to 0.02 rpm above 2 Hz (i.e. 60 rpm for the 4 pole machine). A significant aspect of the research has been the mathematical derivation of the speed bandwidth limitations for both sensored and sensor less drives, thus allowing for quantitative comparison of their dynamic performance. It has been found that the speed bandwidth limitation for sensor less drives depends on the accuracy to which the machine parameters are known and that for maximum dynamic performance it is necessary to tune the flux and speed estimator against variations in stator resistance in addition to the tuning mechanism deriving from the DFT speed detector. New dynamic stator resistance tuning algorithms have been implemented. The resulting sensor less drive has been found to have a speed bandwidth equivalent to sensored drives fitted with medium resolution encoders (i.e. about 500 ppr), and a zero speed accuracy of ±8 rpm under speed control. These specifications are superior to any reported in the research literature.

Keywords – Measurement, Control, Torque, Induction Machines

I. INTRODUCTION

In present days the 3 phase induction motors are extensively used for various industrial applications because of the following reasons one such way is it can be turned on and the direction of rotation can be reversed. The 3 induction phase motor is accountable for larger load operations in several applications. It is widely used in robotics, used in billet shearing machines, rolling machines. An induction or asynchronous motor is an AC electric motor in which the electric current in the rotor needed to produce torque is obtained by Electro Magnetic Induction

from the magnetic field or the stator winding. The speed control of induction motor is done at the cost of decrease in efficiency and low electrical power factor. In 3 phase induction motor the speed control plays a very important role hence it can be done by some of the following ways, one is by rotor side and other is by stator side. From stator side is by (i) Variable frequency control. (ii) Changing the number of stator poles. (iii) Controlling supply voltage. (iv) Adding rheostat in the stator circuit. From the rotor side is done by (i) Adding the external resistance on the rotor side (ii) Cascade control method. (iii) Injecting slip frequency EMF into rotor side. The voltage source inverters produce an output voltage or a current with levels either 0 or ± v dc. They are known as the two level inverter. This output is not a sinusoidal wave. To obtain near sinusoidal wave using multilevel inverter. The multilevel inverters have drawn tremendous interest in the power industry they present a new set of features that are well suited for use in reactive power compensation it may be easier to produce a high power ,high voltage inverter with the multilevel structure because of the way in which device voltage stresses are controlled in the structure increasing the number of voltage levels in the power rating the in the unique structure of multilevel voltage source inverters allows them to reach high voltages with low harmonics without the use of transformers or series connected synchronized switching device. As the number of voltage levels increases the harmonics content of the output voltage waveform decreases significantly.

II. BLOCK DIAGRAM

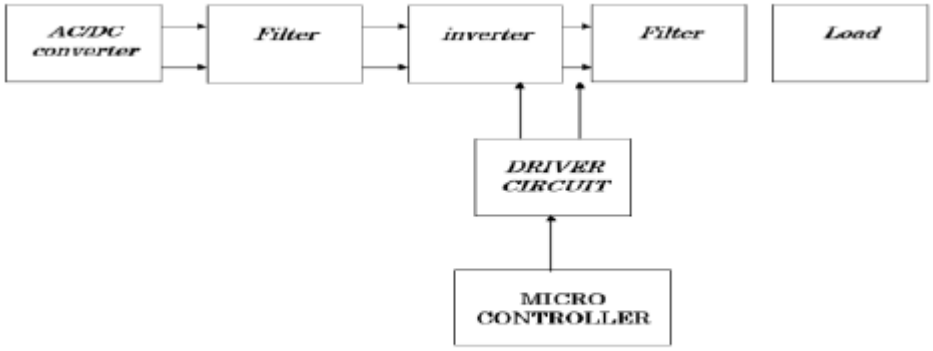

Fig 1: Block Diagram

The induction motor is fed using a commercial IGBT voltage fed inverter rated 10 kW. The inverter has been modified to allow for external PWM to be fed directly to the base drivers of the transistors. A dynamic braking unit, together with dynamic braking resistors, has been fitted in order to dissipate the energy generated by the induction motor during deceleration.

III. Proposed Methodology

A. Indirect Rotor Field Orientation (IRFO): This method of field orientation was proposed as early as the late sixties [3], and is based on imposing the required slip into the machine so that rotor field orientation is forced. Using rotor flux and stator currents as state variables, and assuming a synchronous frame of reference aligned with the rotor flux ($\lambda rq = 0$), we have

$$v_{sd} = R_s i_{sd} + \sigma L_s p i_{sd} - \omega_e \sigma L_s i_{sq} + \frac{L_0}{L_r} p \lambda_{rd} \quad (3.1)$$

$$v_{sq} = R_s i_{sq} + \sigma L_s p i_{sq} + \omega_e \sigma L_s i_{sd} + \omega_e \frac{L_0}{L_r} \lambda_{rd} \quad (3.2)$$

$$\lambda_{rd} = \frac{L_0 i_{sd}}{1 + T_r p} \quad (3.3)$$

$$\omega_{sl} = \frac{L_0 R_r}{L_r \lambda_{rd}} i_{sq} \quad (3.4)$$

$$v_{sd} = R_s i_{sd} + \sigma L_s p i_{sd} - \omega_e \sigma L_s i_{sq} \quad (3.5)$$

$$v_{sq} = R_s i_{sq} + \sigma L_s p i_{sq} + \omega_e L_s i_{sd} \quad (3.6)$$

$$\lambda_{rd} = L_0 i_{sd} \quad (3.7)$$

$$\omega_{sl} = \frac{i_{sq}}{T_r i_{sd}} \quad (3.8)$$

This implementation uses fast current loops so the machine appears current fed and hence the stator dynamics can be neglected. Due to the high bandwidth of the current controllers, reference currents can be used instead of the measured ones for the calculation of the machine slip.

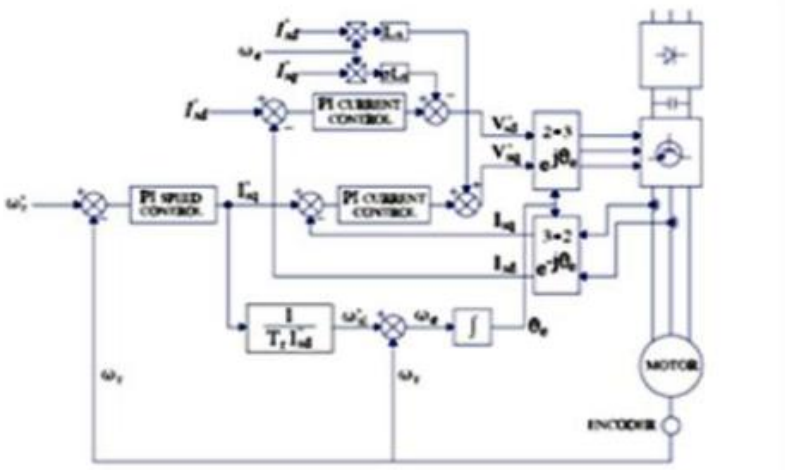

Fig:2 Indirect Rotor Flux Orientation Implementation

Correct field orientation is only dependent on the rotor time constant (Tr) and that the rotor flux is independent of the q-axis current. Since simple techniques of Tr adaption have been devised [4] this method of field orientation can be considered very effective. Field orientation is kept regardless of the rotational speed of the machine and therefore IRFO can be used at standstill. This system provides a good torque response, due to the high bandwidth of the current controllers. B. Direct Stator Field Orientation (DSFO): The dynamic equations of the induction machine in a synchronous rotating frame aligned with the stator flux ($\lambda sq = 0$) can be expressed as follows

$$v_{sd} = R_s i_{sd} + \frac{d}{dt}\lambda_{sd}$$
$$v_{sq} = R_s i_{sq} + \omega_e \lambda_{sd} \qquad (3.9)$$

$$0 = (1 + T_r p)\lambda_{sd} - (L_s + \sigma L_s T_r p) i_{sd} + \omega_s \sigma L_s T_r i_{sq} \qquad (3.10)$$

$$0 = -(L_s + \sigma L_s T_r p) i_{sq} - \omega_s \sigma L_s T_r i_{sd} + \omega_s T_r \lambda_{sd} \qquad (3.11)$$

From (3.11) an expression to determine the slip frequency is derived

$$\omega_{sl} = \frac{(1 + \sigma T_r p) L_s i_{sq}}{T_r(\lambda_{sd} - \sigma L_s i_{sd})} \qquad (3.12)$$

From (3.10) follows that the flux magnitude depends on both isd and isq. This is undesirable and a compensation term (idq) is calculated to decouple the flux from the torque producing current. Rearranging (3.10)

$$\lambda_{sd} = \frac{(1 + \sigma T_r p) L_s}{(1 + T_r p)} \left(i_{ds} - \frac{\sigma T_r \omega_s}{(1 + \sigma T_r p)} i_{sq} \right) \qquad (3.13)$$

Hence

$$i_{dq} = \frac{\sigma T_r \omega_s}{(1 + \sigma T_r p)} i_{sq} \qquad (3.14)$$

Substituting ωs with its value from (3.12)

$$i_{dq} = \frac{\sigma L_s}{(\lambda_{sd} - \sigma L_s i_{sd})} i_{sq}^2 \qquad (3.15)$$

The stator flux angle required for field orientation can be obtained from a direct measurement of the flux (using Hall probes [6], tapped windings, saturation effects [4], etc.) or by calculating the flux from the back e.m.f of the machine

$$\underline{\hat{\lambda}}_s = \int (\underline{v}_s - \hat{R}_s \underline{i}_s) dt \qquad (3.16)$$

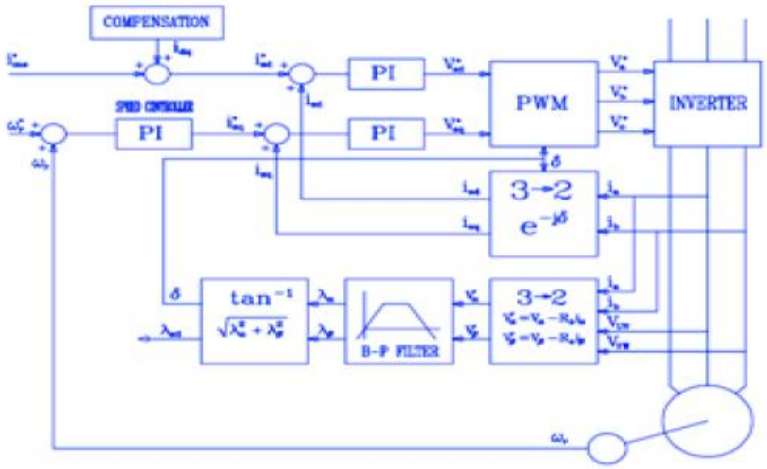

Fig 3: Basic Direct Stator Flux Orientation Scheme

A typical implementation of a DSFO drive is shown in Fig. Note a band pass filter has been used instead of a pure integral, to avoid integrator drift problems. Therefore the DSFO implementation can only be used above a certain frequency which is slightly higher than the band pass filter cut-off frequency.Moreover flux orientation depends on the stator resistance Rs. The sensitivity to the stator resistance is frequency dependent; the voltage drop across Rs is negligible at high speed when compared with the back e.m.f. but at low speeds the term Rsis will be of the same order of magnitude as the back e.m.f. Therefore good field orientation at low speed can only be achieved if the stator resistance is known with high accuracy. This is difficult to accomplish since Rs varies noticeably with temperature. Note also the cross coupling term in the flux equation (3.13). This term causes the actual flux in the machine to drop when the magnitude of isq increases. In Fig. a compensation term is added to the isd demand to cancel this cross coupling. However the practical cancellation of the cross-coupling term is difficult, since it requires a very accurate knowledge of all the magnitudes in (3.15). For instance, for the 4 kW machine considered in this study, isd = 2.2 A and isq = 6 A during a speed transient. A 10% error on σLs (typically 70 mH) would cause an error of 3.6 A in isd. The fact that σLs is dependent on isq, especially in closed slot machines, contributes to exacerbate the sensitivity of the compensation term to changes in σLs.

C. Direct Rotor Field Orientation (DRFO):

In a DRFO system, the rotor flux vector is computed directly for field orientation. The dynamic equations of the induction machine in a synchronous frame aligned with the rotor flux are the same as for the IRFO. However, no forcing condition is used for field orientation. The main advantage of rotor flux orientation (i.e. decoupled control of isq and flux) is retained with a DRFO system. The implementation of a DRFO based on a flux observer I shown in Fig. Speed feedback could be obtained from a transducer or from a speed observer.

Computation of the rotor flux (or rotor angle) for field orientation from terminal quantities of the machine is normally preferred to searching methods based on Hall sensors [6], tapped windings [2] or similar methods that require special modification of the machine. A review of several methods of rotor flux estimation of standard induction machines (i.e. without requiring special modification of the machine). Most of these methods can be easily modified to provide a stator flux estimate rather than rotor flux, retaining most of their characteristics (parameter

sensitivity, speed range, etc). However rotor flux orientation has been generally preferred in sensorless drives because of the inherent decoupling of isq and flux in the rotor frame.

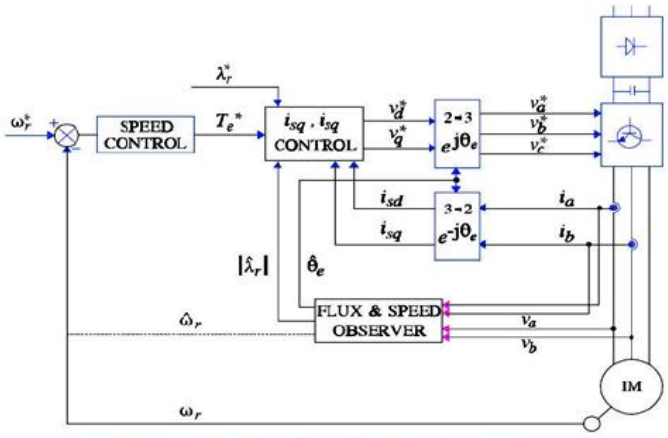

Fig.4: Direct Rotor Flux Orientation Diagram

D. Rotor Flux Observers for DRFO:

Open Loop Observers: The rotor flux can be calculated by using the stator equation of the induction machine

$$\underline{\lambda}_r = \int (\underline{v}_s - R_s \underline{i}_s)\,dt - \sigma L_s \underline{i}_s \qquad (3.17)$$

This expression is also known as the voltage model of the machine. It presents similar problems and advantages as the DSFO described previously, since it requires a pure integration for flux estimation and it is sensitive to errors in the stator resistance at low speed. This makes the voltage model unsuitable for low speed operation. However, it does not require the rotor speed to produce a flux estimate. Unlike the DSFO, there is no cross coupling between isq and λrd, due to the orientation on the rotor flux. On the other hand field orientation in the DRFO depends on σLs. However this higher acceleration torque is obtained with a higher isd (needed to keep the stator flux constant), and therefore there is more power going into the machine in the DSFO case than in the DRFO implementation. Rotor flux can also be obtained from the rotor equations of the machine.

$$\underline{\lambda}_r = \frac{L_0}{T_r}\underline{i}_s - \left(\frac{1}{T_r} - j\omega_r\right)\underline{\lambda}_r \qquad (3.18)$$

Known as the current model. This model has similar advantages and disadvantages to the IRFO implementation. It requires knowledge of the rotor speed and it is dependent on the rotor time constant. The current model sensitivity to Tr is independent of the machine speed and a good degree of field orientation can be achieved even at stand-still, with appropriate speed measurement. The performance of this system degrades during field weakening, due to the difficulty of determining Tr and L0 with changing flux. In fact, a DRFO implementation based on the current model with speed transducer yields identical performance to that of Indirect Rotor Flux Orientation.

Closed Loop Flux Observer: The advantages of both current and voltage models can be combined in what is known as a Closed Loop Flux Observer (CLFO) [3]. The structure of this observer is shown in Fig.

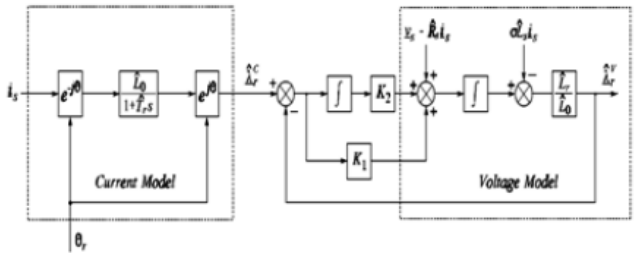

Fig 5: Closed Loop Flux Observer

The CLFO consists of the two models, based on (3.17) and (3.18), and connected by a PI controller. Note the current model has been expressed in rotor coordinates rather than in stator fixed coordinates. The values K1 and K2 of the PI controller are designed to obtain a close loop bandwidth in the voltage model of ωcpl (typically 1 or 2 Hz). For frequencies below ωcpl, the CLFO output (λV) follows the flux r estimate from the current model (λ C). For frequencies above ωcpl (outside the r bandwidth of the PI controller), the two models are not coupled any more. Therefore the output λ V corresponds to that of the voltage model. This behaviour can also be understood from the overall CLFO transfer function

$$\underline{\lambda}_r^V = K_p \frac{L_r}{L_0} \frac{(s+a)}{s^2 + K_p \frac{L_r}{L_0} s + K_p \frac{L_r}{L_0} a} \underline{\lambda}_r^C + \frac{s^2}{s^2 + K_p \frac{L_r}{L_0} s + K_p \frac{L_r}{L_0} a} \frac{L_r}{L_0} \left(\frac{1}{s} (\underline{u}_s - R_s \underline{i}_s) - \sigma L_s \underline{i}_s \right) \quad (3.19)$$

where the PI controller is expressed as Kp(s + a)/s. The first term of the transfer function corresponds to a low pass filter applied to the output of the current model. The second term is equivalent to a high pass filter applied to the flux estimate obtained from direct integration of the stator back e.m.f. The equivalent diagram of the CLFO is shown in Fig. The cut off frequency of both filters (ωcpl) is the same and provided that a > ωcpl the resulting phase shift of the combined filters is very close to zero for the whole range of frequencies.

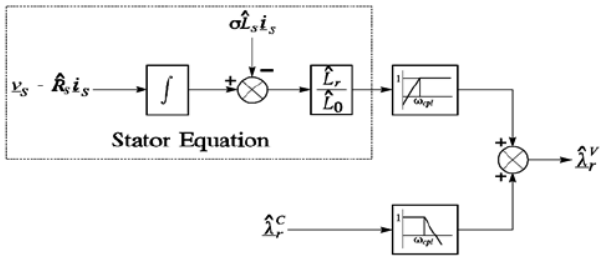

Fig 6: Equivalent diagram of the closed loop flux observer

Therefore the CLFO can operate properly at zero speed, due to the use of the current model which offers the same performance as indirect rotor field orientation. Figure shows a speed reversal transient using a CLFO-DRFO implementation. This transient shows a very good field orientation, and it is almost identical to the IRFO speed reversal shown in Fig. The only difference is the small spike in the isd current at the beginning of the transient in Fig caused by the fact that the IRFO ωsl calculator uses the reference value of isq and the actual isq takes a small time to respond to changes in isq*.

Speed Observers:

Some sort of speed estimation is needed for speed and/or field orientation of sensorless induction motor drives. Different kinds of speed estimators have been developed, using techniques such as open loop slip calculation, Extended Kalman Filters, Luenberger observers, Least Squares Regression Models, or Model-Reference Adaptive Systems (MRAS). Open loop slip calculation is relatively easy to implement. The stator frequency (ωe) can be calculated using

$$\omega_e = \frac{\underline{\lambda}_s \times (\underline{v}_s - R_s \underline{i}_s)}{|\underline{\lambda}_s|^2} \qquad (3.20)$$

The excitation frequency (ωe) can also obtained by differentiating the flux angle or directly from the control system in the case of IRFO. The calculation of the slip can be carried out by using

$$\omega_{sl} = \frac{(1 + \sigma T_r s) L_s i_{sq}}{T_r (\lambda_{sd} - \sigma L_s i_{sd})} \qquad (3.21)$$

and assuming λsq = 0 (Stator Field Orientation SFO). Assuming Rotor Flux Orientation (RFO), the machine slip can also be calculated by [5]

$$\omega_{sl} = \frac{i_{sq}}{T_r \, i_{sd}} \qquad (3.22)$$

A system that calculates the rotor speed of the machine based on the above expressions is bound to be extremely sensitive to parameter errors and in some cases very noisy. Equation (3.20) requires knowledge of the stator flux. Calculation of the stator flux from the voltage model is sensitive to stator resistance errors. Moreover, (3.20) itself depends on Rs, so that this method of calculating ωe is bound to be very inaccurate at low speed. The alternative of calculating ωe by direct differentiation of the flux angle is bound to be noisy. Moreover, slip calculation based either on (3.21) or (3.22) depends strongly on an accurate knowledge of the machine parameters and also on good field orientation. An experimental result of open loop speed estimation using (3.21) is shown in Fig. During deceleration the speed error is about 35 rpm. At speeds close to zero, the estimate is extremely poor, due to the low frequency limitation of the ωe calculation based on (3.20). Typical steady state error at full load is approximately 20 to 25 rpm. These figures represent 25 to 30% rated slip (80 rpm). Therefore speed holding and speed accuracy at medium/low speed is very poor. In conclusion, open loop speed calculation can only be used in very low performance applications in which speed accuracy and speed holding capability are not important.

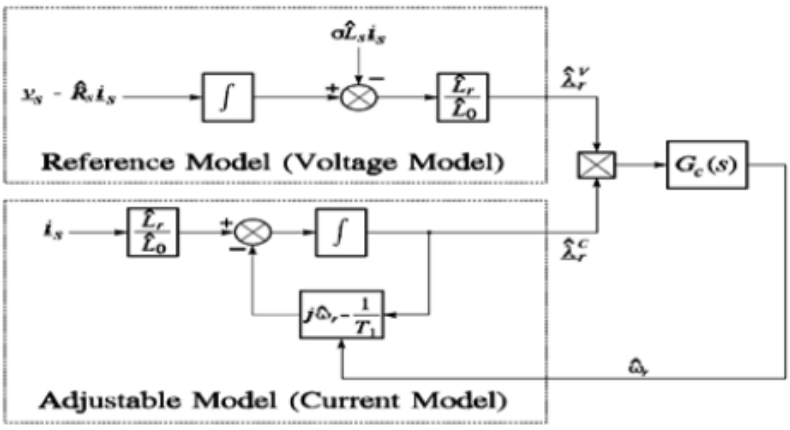

Fig7: Basic MRAS Speed identification using the rotor flux as error vector

A basic MRAS implementation using the rotor flux as error vector is shown in Fig. This system is based on the fact that the rotor flux can be obtained from either the voltage or current model. The flux estimate produced by the former (λVr), does not depend on the rotor speed, and is used as a reference model. The latter produces a flux estimate (λCr) that is dependent on the rotor speed. Therefore the rotor speed in the current model can be adjusted to force an error function between the estimated fluxes to zero. The loop that drives this error function to zero is termed the speed adaption loop, and the function Gc(s) is known as the adaptive controller. Any error function that satisfies the hyperstability criteria (i.e. that results in a stable system) can be chosen. The cross product of the flux estimates has been shown to satisfy the hyperstability criteria [2] and will therefore be used here

$$\varepsilon = \hat{\lambda}_{rd}^{C}\hat{\lambda}_{rq}^{V} - \hat{\lambda}_{rq}^{C}\hat{\lambda}_{rd}^{V} = \left|\hat{\lambda}_{r}^{V}\right|\left|\hat{\lambda}_{r}^{C}\right|\sin\left(\hat{\theta}_{r}^{C} - \hat{\theta}_{r}^{V}\right)$$

Where θc and θV are the rotor flux angles estimated by the voltage and current model respectively. For small differences between estimated flux angles, the error function can be expressed as

$$\varepsilon = \left|\hat{\lambda}_{r}^{V}\right|\left|\hat{\lambda}_{r}^{C}\right|\left(\hat{\theta}_{r}^{C} - \hat{\theta}_{r}^{V}\right) \qquad (3.24)$$

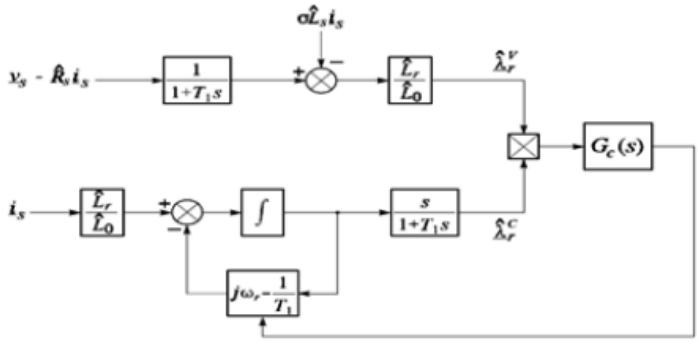

Fig 8: MRAS Speed observer with DC blocking filters

The voltage model obtains the rotor flux by integration so that in practice dc offsets must be removed by employing a dc-blocking filter so that the error vector becomes an ac-coupled rotor flux signal (Fig.) [2-7]. MRAS speed observers using a voltage model with dc- blocking filters present the disadvantage that at low speeds misidentification of Rs and the distorting effects of the dc-blocking filter cause the rotor flux estimate to become inaccurate and both the speed estimate and the field orientation breaks down below 1 or 2 Hz. An improvement in both rotor flux and speed estimate at very low speed may be obtained by using a closed loop flux observer (CLFO) instead of two independent flux models [4].

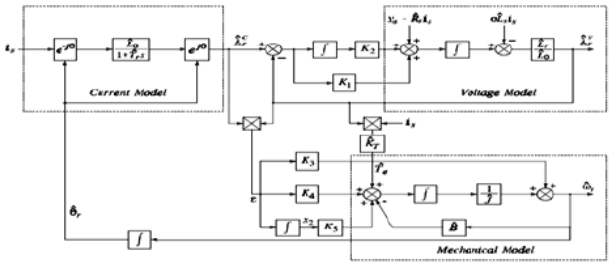

Fig 9: MRAS-CLFO flux and Speed Observer

At frequencies above ωcpl the voltage and model loops are effectively independent and the system is equivalent to the basic MRAS shown in Fig. However, as the frequency approaches zero, λVr=λCr and speed estimate forcing is lost. A mechanical model can compensate for this effect in that flux and speed estimates are produced even when λVr= λCr. The structure of the mechanical model is also shown in Fig. in which an estimated torque signal is used to drive a first order drive train model. This model is also driven by the signal through a PI controller which will help compensate model errors. The feedforward term K3 weights the effect of the pure MRASCLFO and the mechanical model upon ωr. At low frequencies, the MRAS-CLFO is equivalent to the speed observer shown in Fig. Since λVr= λCr. Therefore operation at very low speed is dependent on good knowledge of the mechanical parameters. However, if the mechanical parameters are not accurately known, then the compensation will merely be less effective but still an improvement over the case when no mechanical model is used at all. In practice it is found that field orientation and the speed estimate start to deteriorate for excitation frequencies below ωlim, a frequency slightly higher than ωcpl (eg if ωcpl is designed at 0.8 Hz, ωlim is about 1.5 Hz). The degree of deterioration depends on the accuracy of the of the estimated voltage model and mechanical parameters.

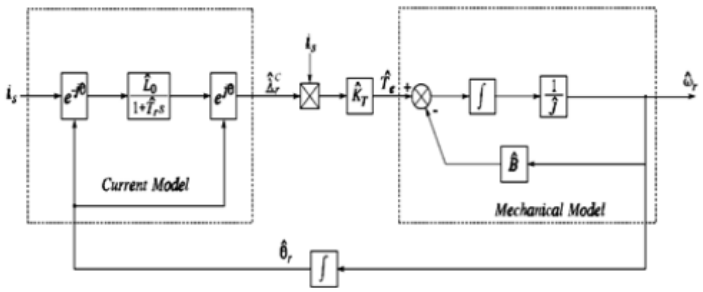

Fig 10: MRAS-CLFO low frequency equivalent diagram

HARDWARE OPEN LOOP MODEL:

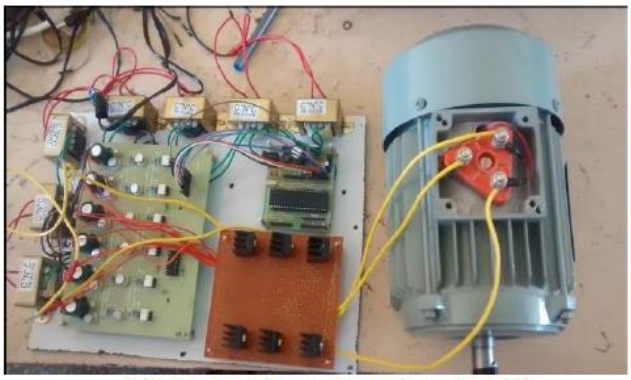

Fig 11: Hardware Open loop Model

CLOSED LOOP SIMULATION MODEL

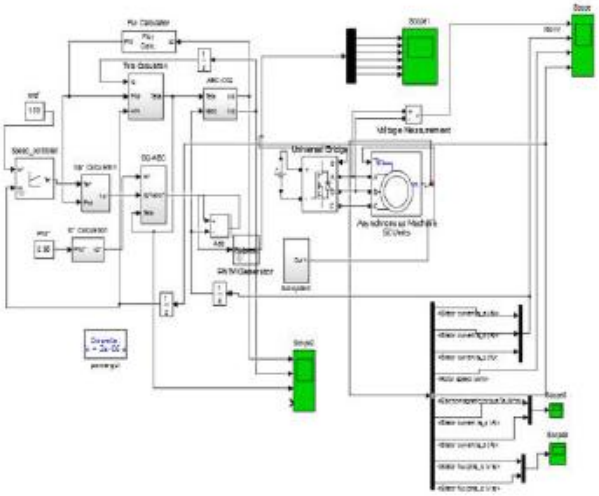

Fig 12: Closed loop Simulation Model

SWITCHING SEQUENCE:

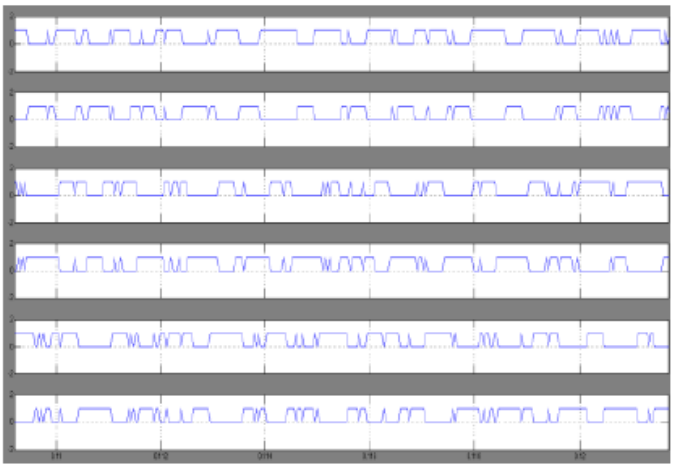

OUTPUT:

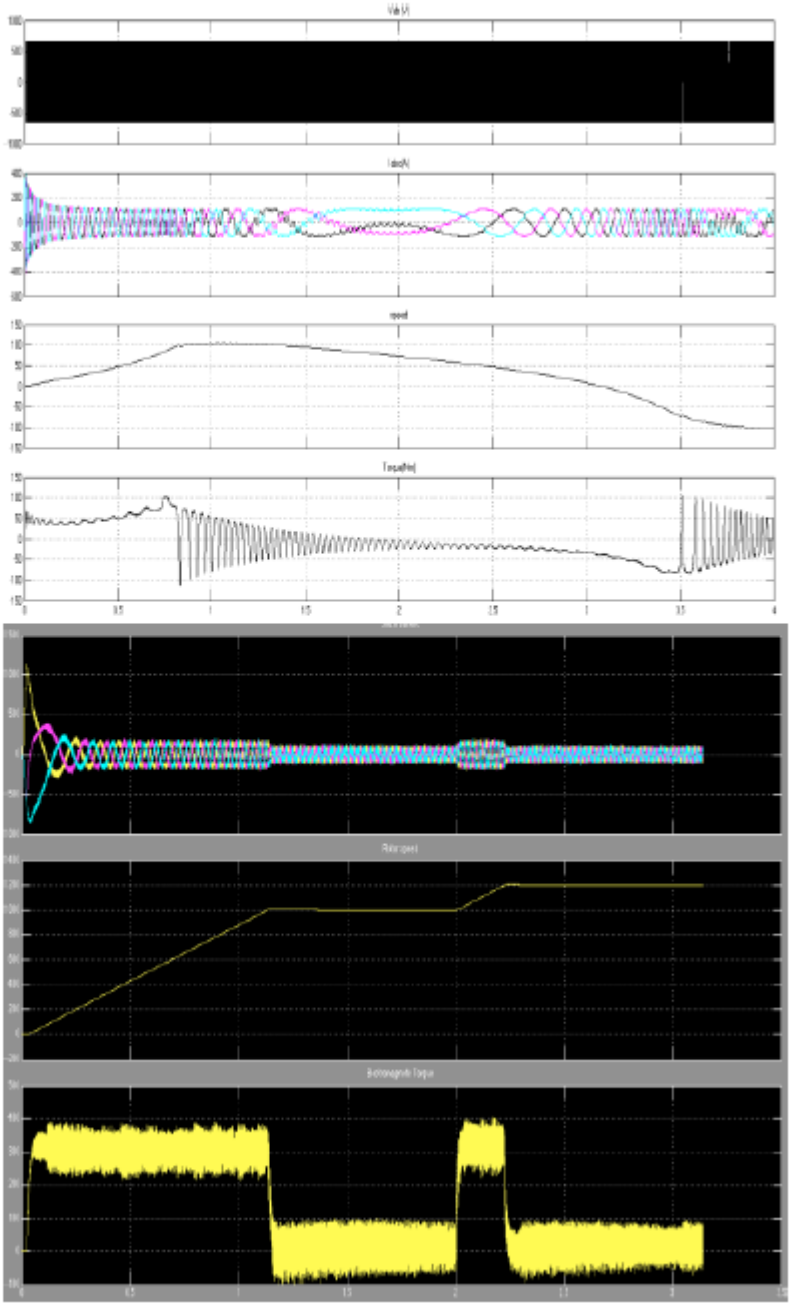

REFERENCES

1. J.Rodrigues, J.S Lai, and F.Z.Peng, "Multilevel inverters: a survey of topologies, controls and applications,"IEEE Trans.Ind.Electron.,vol,no.4 pp.724-738,aug2002.
2. L.M. Tolbert and T.G.Habetler," novel multilevel inverter carrier-based PWM method," IEEE Trans.Ind.Appl., vol.35, no,5.pp 1098-1107, sep/oct.1999.

3. G.S.Perantzakis,F.H.Xepapas,and S.N. Manias,"A new four level PWM inverter topology for high power applications-effects of switching strategies on losses distribution," in Proc.PESC'04, Aachen, Germany, 2004, pp.4398-4404.
4. J.S.Lai and F.Z .Peng, "Multilevel converters-a new breed of power converters," IEEE Trans.Ind.Appl., vol.32, no.3 pp.509-517, may/jun. 1996.
5. G.Carrara, S.Gardella, M.Marchesoni, R.Salutari, and G.Sciuto,"A new multilevel PWM method: a theoretical analysis," IEEE Trans Power Electron., vol.7.no.3,pp.497-505,july.1992.
6. C.Rech., H.Pinherio, H.A.Grundling, H.L.Hey, and J.R.Pin-herio, "Analysies and comparison of hybrid multilevel voltage source inverters," in Proc, IEEE PESC'02,2002,pp.491-496.